

CHAPTER II

LITERATURE REVIEW

2.1 Corrosion of Steel

Corrosion is an important problem common to all nuclear power plants. It causes deterioration of the materials, such as pipes in CANDU reactors, which makes its properties becomes lower than it was.

2.1.1 Definition of Corrosion

Corrosion is defined as the destruction or deterioration of a material because of reaction with its environment like air, moisture, or acid. Practically in a nuclear power plant, they use high temperatures and pressures during power production; these usually involve more severe corrosion conditions and lead to costly repairs for safety reasons, etc. However, some corrosion is beneficial or desirable in some cases, such as chemical machining or chemical milling, where unmasked areas are exposed to acid and excess metal is dissolved. Anodizing of aluminum is another beneficial corrosion process used to obtain better and more uniform appearance from a protective corrosion product on the surface (Fontana, 1986).

2.1.2 Flow-accelerated Corrosion (FAC)

Flow accelerated corrosion (FAC), also sometimes referred to as erosion-corrosion (E/C), is a process whereby the normally protective oxide layer on carbon or low-alloy steel and base metal dissolve into a stream of water or water-steam mixtures, accelerated by flow or flow impingement. FAC causes wall thinning (metal loss) of carbon steel piping, tubing and vessels exposed to flowing water or wet steam. If undetected, the degraded component can suddenly rupture (Dooley and Chexal, 2000; Kain *et al.*, 2011).

In the FAC process, the inside surface of the pipe comes in contact with the solution. The surface is attacked and forms an oxide layer by the reaction between water or dissolved oxygen and steel. As the result of a high flow velocity, some of that oxide layer is dissolved and eroded away and carried with the flow,

likely to deposit elsewhere downstream in the system. As conditions favor the formation of the oxide layer, a new layer will be formed wherever bare metal is exposed, with continuous removal and reforming of the oxide. Consequently, the metal loss continues resulting in the reduction of wall thickness as shown in Figure 2.1 (Silbert, 2002).

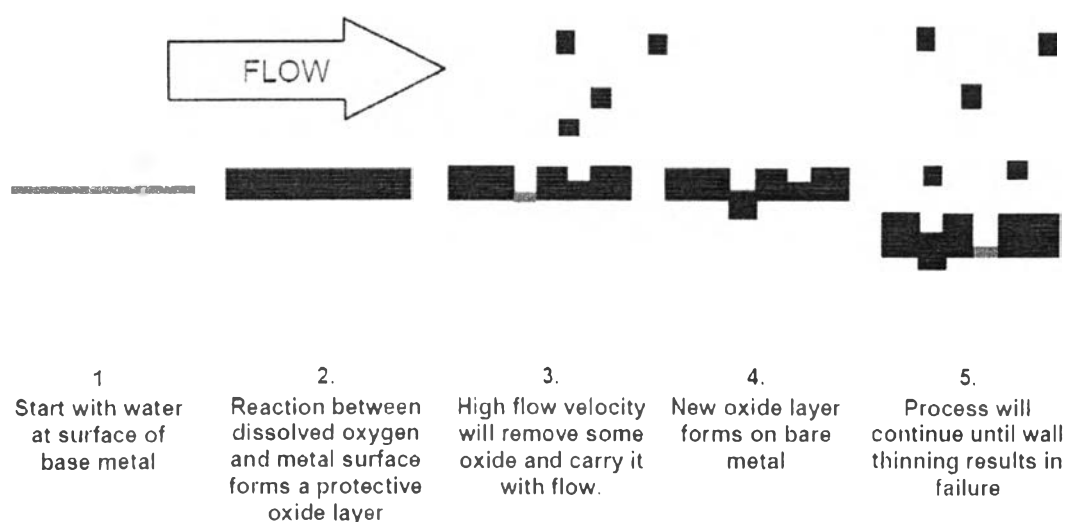


Figure 2.1 Mechanism of FAC (Silbert, 2002).

2.1.3 FAC in the Feeder pipes in CANDU Reactors

The FAC effect can be investigated in the primary heat transfer system of the CANDU reactor. The inlet feeder pipes undergo less FAC than outlet feeder pipes. Because the coolant temperature increases from 265 °C to 310 °C during flow through the reactor core, where there is no source of iron, this results in higher solubility of the oxide film in the outlet feeders. Consequently, the coolant in the inlet feeder pipes is saturated with dissolved iron, which results in a lower corrosion rate and a relatively thick film compared with outlet feeder pipes (Chung, 2010; Lister *et al.*, 1997; Lister *et al.*, 2001; Yuan *et al.*, 2008).

2.2 Mechanism of Oxide Formation and Hydrogen Evolution

The understanding of the phenomena involved on FAC and hydrogen permeation involves linking mechanisms of oxide formation and dissolution with mass transfer.

2.2.1 Magnetite Formation

Magnetite (Fe_3O_4) is the structure of oxide film that is usually present on the surface of the feeder pipe in a CANDU reactor. This oxide generally behaves like a corrosion-resistant layer on the steel. On the outlet feeders, however, it degrades from dissolution and erosion and loses its protective ability.

Moreover, this oxide film also acts as a barrier to hydrogen transportation. In 2009, Leelasangjai investigated hydrogen diffusion through various steels with and without oxide films. The results indicated that the hydrogen pressure inside the carbon steel tube dropped rapidly from 105 to 85 psig after the removal of the oxide film, as shown in Figure 2.2. She suggested that this was because there was no oxide film to act as a barrier to hydrogen transportation (Leelasangjai, 2009).

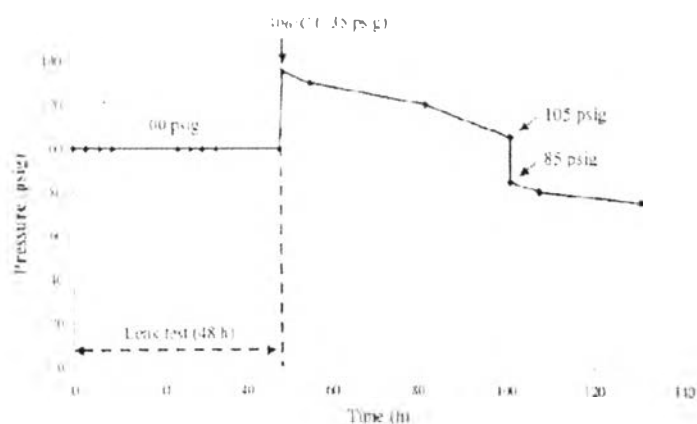


Figure 2.2 The change in hydrogen pressure inside the carbon steel tube with time after the removal of the oxide film formed on the outside surface (Initial hydrogen pressure: 100 psig at 25 °C. Set point temperature: 310 °C. Tube temperature: 306 °C) (Leelasangjai, 2009).

Normally, carbon steel corrodes in high temperature water and forms a double oxide layer known as the Potter-Mann layer. The inner layer consists of small magnetite crystals that grow at the metal-oxide interface, replacing the corroded volume (Potter and Mann, 1962). This layer is compact and adherent (Potter and Mann, 1963) since it nucleates in the limited space. The outer layer consists of larger magnetite crystals that grow from solution (Lang, 2000) since it grows without space limitation. A schematic of the double oxide layer formed on carbon steel is shown in Figure 2.3.

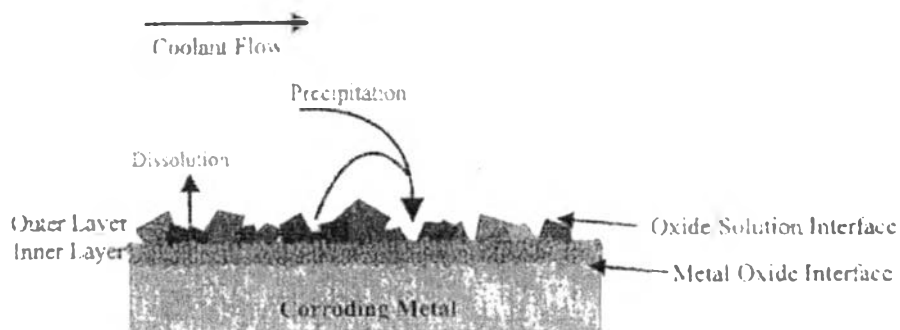


Figure 2.3 Schematic of double oxide layer formed on carbon steel (Kongvarhodom, 2014).

The corrosion of carbon steels and low alloy steels in high-temperature water, in the absence of oxygen, involves the transport of oxygen-bearing species to the metal/oxide interface and the outward movement of metal ions to the solution phase. When the solution phase becomes saturated with soluble iron, an outer magnetite layer is nucleated and grows on the surface. The net result is a double magnetite layer (Cheng and Steward, 2004).

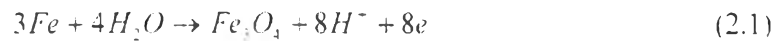
2.2.2 Hydrogen Evolution

Cheng and Steward (2004) investigated the oxygen-bearing species in high temperature deaerated alkaline solution. They proposed that in the absence of oxygen, the inward movement of oxygen-bearing species occurs by diffusion of either water molecules or oxygen ions or hydroxide ions. Oxygen ions involve the

formation of oxide film only after a sufficiently anodic potential is imposed and a deprotonation of H_2O takes place, resulting in the loss of protons to the solution and oxygen ions migrating towards the steel surface. Therefore, oxygen ions cannot be the diffusion species in the reported experiments.

Considering the thin oxide film, the electric charge strength across the film is very high. The established electric field will block the negatively charged ions, such as OH^- from moving towards the steel surface. This eliminates hydroxide ions as the diffusion species. Therefore, the oxygen-bearing species involving the formation of the magnetite layer must be water.

A schematic view of the magnetite film formed on a steel surface in high temperature water solution is shown in Figure 2.4. Water molecules diffuse through the inner oxide layer and react directly with steel at the steel/oxide interface. Iron dissolution occurs where no oxide layer exists. Protons at the oxide/water interface diffuse through the oxide layer under the concentration and potential gradients and discharge as hydrogen atoms at the steel/oxide interface. The relevant reactions occurring at the steel/oxide interface are shown in Equations 2.1-2.3.



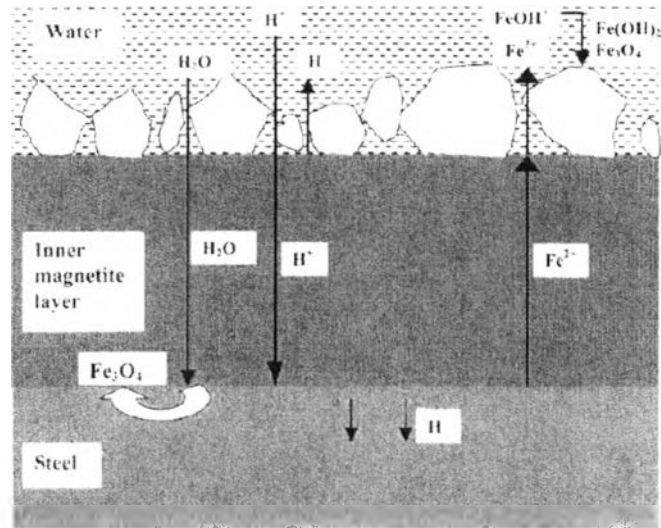
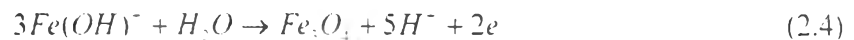


Figure 2.4 Schematic view of the formation mechanism of the magnetite film on the steel surface in high temperature water (Cheng and Steward, 2004).

The ferrous ions diffusing out of the oxide layer and existing as $\text{Fe}(\text{OH})^+$ in high temperature water must stabilize themselves by decreasing their charge/radius ratios through hydrolysis to form hydrous iron ions. The hydrous iron ions will deposit as loose $\text{Fe}(\text{OH})_2$ once the saturation of iron ions is achieved. The outer deposition of the magnetite layer is then formed in high-temperature water, accompanying the discharge of hydrogen ions. Therefore, the electrochemical reactions occurring at the oxide/water interface are:



As in Equations 2.4 and 2.5, these reactions indicate that magnetite and hydrogen is produced by the carbon steel corrosion process.

2.2.3 Hydrogen Emission During Steel Corrosion

Tomlinson (1981) studied the hydrogen emission from the oxidation of steel in high-temperature water. He reported that protons produced from the corrosion process diffuse in both directions across the oxide, with the direction and magnitude of the proton flux being dependent on the structure of the oxide layer.

Hydrogen atoms are formed at both the metal/oxide interface and the oxide/water interface. At the oxide/water interface, hydrogen atoms are either discharged by electron diffusion across the oxide or diffuse through the oxide as protons which are discharged at the metal/oxide interface. Under the concentration and potential gradient, protons at the oxide/water interface diffuse rapidly through the oxide layer and discharge as hydrogen atoms at the metal/oxide interface.

The experimental evidence indicates that up to 90 % of the hydrogen atoms are generated at the metal/oxide interface during the corrosion of carbon steels by high temperature deaerated water. More than 99 % of these hydrogen atoms will diffuse through the steel at the temperature of interest since it is generally accepted that the hydrogen diffusivity in an oxide film is low. Hydrogen diffuses through the metal 330 times more rapidly than through the oxide (Tomlinson, 1981; Tomlinson and Cory, 1989). It is suggested that if the ratio of the rate of growth of the inner layer to the rate of growth of the outer layer is constant, then the ratio of hydrogen emission from metal and oxide surfaces should also be constant. Furthermore, the fraction of hydrogen passing through the steel appears to increase with the amount of oxide deposited on the tube surface (Tomlinson, 1981; Tomlinson and Cory, 1989).

2.3 Fundamental Law of Diffusion

Diffusion is the movement of a chemical species from a region of high concentration to a region of low concentration (Bird *et al.*, 2001). It is the phenomenon of material transport by atomic motion, which means no fluid motion.

In solid diffusion mechanisms, there are several ways by which the diffusion of atoms in solids might occur. The most important are vacancy diffusion and interstitial diffusion (Hannay, 1967). Vacancy diffusion is a mechanism involving the interchange of an atom from a normal lattice position to an adjacent vacant lattice site or vacancy, as represented in Figure 2.5a. This process necessitates the presence of vacancies, and the extent to which vacancy diffusion can occur is the function of the number of these defects that are present. The second type of diffusion involves atoms migrating from an interstitial position to a neighboring one that is empty. This mechanism is found for interdiffusion of impurities such as hydrogen,

nitrogen, and oxygen, which have atoms that are small enough to fit into the interstitial position. Host or substitutional impurity atoms rarely form interstitials and do not diffuse via this mechanism. This phenomenon is termed interstitial diffusion (Figure 2.5b) (Callister, 1991).

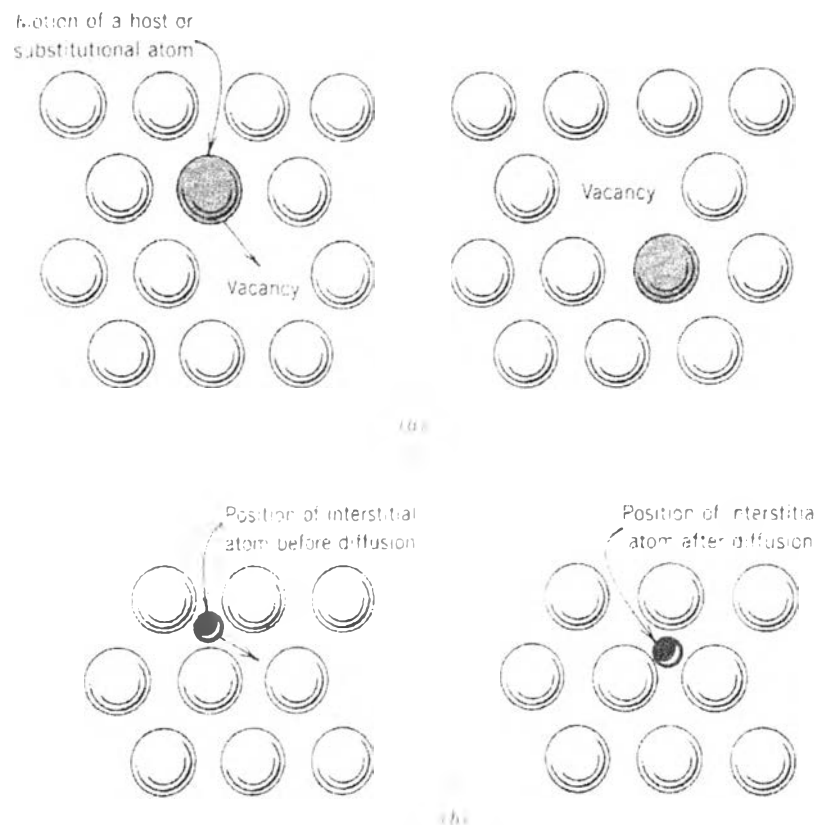


Figure 2.5 Schematic representation of (a) vacancy diffusion and (b) interstitial diffusion (Callister, 1991).

2.3.1 Fick's Law of Diffusion

Fick's Laws of diffusion describe mathematically the diffusion process.

2.3.1.1 *Fick's First Law*

Diffusion is a time-dependent process. The quantity of an element that is transported within another is a function of time. Often, it is necessary to know diffusion flux (J) which is the rate of mass transfer. If the diffusion flux does

not change with time, a steady-state exists. Fick's First Law is used for steady-state diffusion like this. The mathematical equation of steady-state diffusion in a single (x) direction is given by Equation 2.6.

$$J = -D \frac{dC}{dx} \quad (2.6)$$

where:

J is the diffusion flux, which refers to mass, atoms or amount of substance diffusing through and perpendicular to a unit cross-sectional area of solid per unit of time in dimensions of [(amount of substance) length⁻² time⁻¹]. An example is $(\text{mol}/\text{m}^2\text{s})$.

D is the diffusion coefficient or diffusivity in dimension of [length² time⁻¹] which is normally expressed in square meters per second. (m^2/s)

C is the concentration of the diffusing substance in dimensions of [(amount of substance) length⁻³]. An example is (mol/m^3) .

x is the coordinate chosen perpendicular to the reference surface in dimensions of [length]. An example is (m) .

The negative sign indicates that the direction of diffusion is from a high to a low concentration.

The diffusion coefficient is proportional to the diffusing particle velocity, which is a function of the viscosity of the fluid, temperature, pressure and concentration. In steady state, Fick's First Law can be integrated to give Equation 2.7.

$$J = -D \frac{(C_A - C_B)}{x_A - x_B} = -D \frac{(C_A - C_B)}{l} \quad (2.7)$$

where C_A and C_B are the concentration of penetrant at the feed and permeate sides, respectively, and l is the thickness of the diffusion path.

Sometimes the driving force is used in the context of what compels a reaction to occur. For diffusion reactions, several such forces are possible:

but when the diffusion is according to Equation 2.6, the concentration gradient, which is $\frac{dC}{dx}$, is the driving force (Callister, 1991).

2.3.1.2 Fick's Second Law

Under conditions of non-steady state, the diffusion flux and the concentration gradient at some particular point in a solid vary with time, with a net accumulation or depletion of the diffusing species resulting. Equation 2.6 is then no longer convenient; instead, the partial differential Equation 2.8, known as Fick's Second Law, is used.

$$\frac{\partial C}{\partial t} = \frac{\partial}{\partial x} \left(D \frac{\partial C}{\partial x} \right) \quad (2.8)$$

where:

C is the concentration of the diffusing substance in dimensions of [(amount of substance) length⁻³]. An example is $\left(\frac{\text{mol}}{m^3}\right)$.

t is time in dimensions of [time]. An example is (s).

D is the diffusion coefficient or diffusivity in dimension of [length² time⁻¹] which is normally expressed in square meter per second. $\left(\frac{m^2}{s}\right)$

x is the coordinate chosen perpendicular to the reference surface in dimensions of [length]. An example is (m).

The following can be derived from the Fick's First Law and a mass balance and become Equation 2.9:

$$\frac{\partial C}{\partial t} = -\frac{\partial J}{\partial x} = \frac{\partial}{\partial x} \left(D \frac{\partial C}{\partial x} \right) \quad (2.9)$$

If the diffusion coefficient (D) is independent of composition,

Equation 2.9 can be simplified to Equation 2.10 (Callister, 1991).

$$\frac{\partial C}{\partial t} = \frac{\partial}{\partial x} \left(D \frac{\partial C}{\partial x} \right) = D \frac{\partial}{\partial x} \frac{\partial C}{\partial x} = D \frac{\partial^2 C}{\partial x^2} \quad (2.10)$$

2.3.2 Arrhenius Equation

The temperature dependence of the diffusion coefficient is of great importance. The Arrhenius equation is an expression for the temperature dependence of the rate constant of chemical reactions based on the absolute temperature and activation energy. The Arrhenius equation is often used to find the temperature dependence of the diffusion coefficient in as shown in Equation 2.11 (Hannay, 1967).

$$D = D_0 e^{-\frac{\Delta H}{RT}} \quad (2.11)$$

where:

D is the diffusion coefficient or diffusivity in dimensions of [length² time⁻¹] which is normally expressed in square meter per second.

$$\left(\frac{m^2}{s}\right)$$

D_0 is a temperature-independent pre-exponential or the maximum diffusion coefficient (at infinite temperature) in dimensions of [length² time⁻¹]. An example is $\left(\frac{m^2}{s}\right)$.

ΔH is the activation energy for diffusion in dimensions of [energy (amount of substance)⁻¹]. An example is $\left(\frac{J}{mol}\right)$. Some texts use E_A instead of ΔH .

T is the absolute temperature in dimensions of [absolute temperature]. (K)

R is the gas constant in dimensions of [energy temperature⁻¹ (amount of substance)⁻¹]. An example is $\left(\frac{J}{mol \cdot K}\right)$.

Taking natural logarithm of Equation 2.11 yields Equation 2.12.

$$\ln D = \ln D_0 - \frac{\Delta H}{R} \left(\frac{1}{T}\right) \quad (2.12)$$

Since D_0 , ΔH , and R are all constants, this expression takes the form of an equation of straight line as shown in Equation 2.13.

$$y = b + mx \quad (2.13)$$

where y and x are analogous, respectively, to the variables $\ln D$ and $1/T$. Thus, if $\ln D$ is plotted versus the reciprocal of the absolute temperature, a straight line should result, having slope and intercept of $-\Delta H/R$ and $\ln D_0$, respectively (Figure 2.6). This is, in fact, the manner in which the values of ΔH and D_0 are determined experimentally (Callister, 1991).

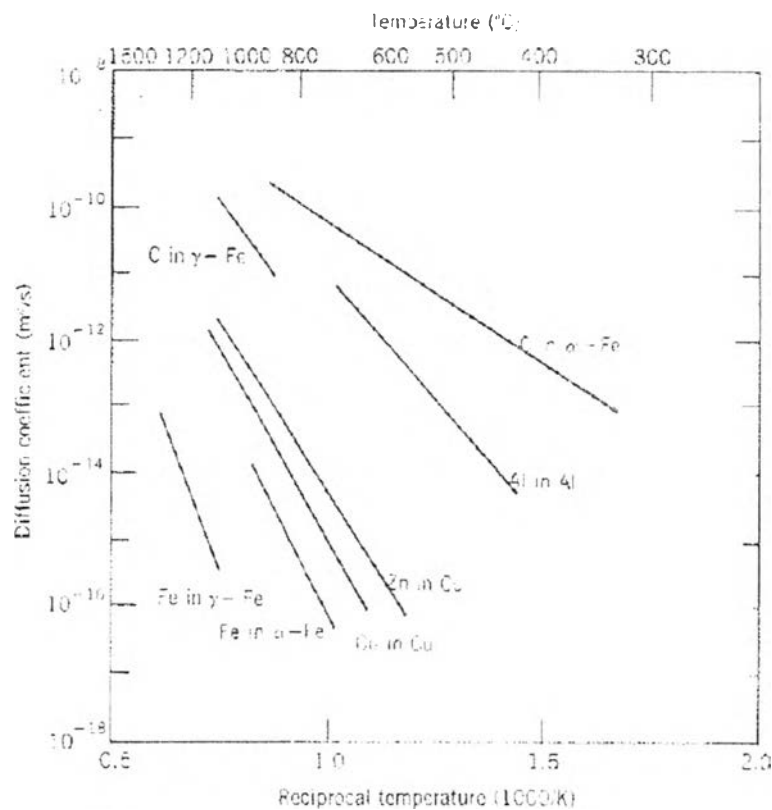


Figure 2.6 Plot of the logarithm of the diffusion coefficient versus the reciprocal of absolute temperature for several materials (Callister, 1991).

Solubility (S) and permeability (P) are temperature-dependent like the diffusivity and can be represented by an Arrhenius equation as shown in Equations 2.14-2.16.

$$S = S_0 e^{-\frac{H_s}{RT}} \quad (2.14)$$

$$P = P_0 e^{-\frac{E_p}{RT}} \quad (2.15)$$

where:
$$P = SD \quad (2.16)$$

2.3.3 Sievert's Law

Hydrogen permeation through membranes has been modeled using the solution-diffusion approach, in which the hydrogen molecules dissociatively adsorb on the metal surface, absorb into and diffuse through the bulk metal in atomic H form, and recombine and desorb as H₂ at the permeate side. When diffusion of hydrogen atoms through the bulk metal is the rate limiting step, hydrogen permeation flux at steady state, J (mol/m² s), can be described by Sieverts' Law:

$$J = \frac{Q}{l} \left(\sqrt{P_{H_2, f}} - \sqrt{P_{H_2, p}} \right) \quad (2.17)$$

In this equation Q is the permeability of hydrogen through membrane (mol/m s Pa^{0.5}), l is the membrane thickness (m), and $P_{H_2, f}$ and $P_{H_2, p}$ are the feed and permeate side partial pressures of hydrogen, respectively. The derivation of Sieverts' Law also assumes that the surface coverage of H at both the feed and permeate sides of the membrane is in equilibrium with the respective fluid phases, and that the adsorption equilibrium constant is the same on both sides as shown in Equation 2.18.

$$C = K P_{H_2}^{0.5} \quad (2.18)$$

where C is the atomic hydrogen concentration on the membrane surface, K is the dissociative adsorption equilibrium constant and P_{H_2} is the hydrogen partial pressure. The 0.5 exponent comes from dissociative adsorption of a diatomic molecule, and this is where the square root comes from in the flux equation above. Sieverts' Law is widely applied in analyzing hydrogen permeation through membranes, even in some cases where the assumptions made in deriving Sieverts' Law are not valid (Al Raisi and Gardner, 2007).

Equation 2.17 can also be expressed as Equation 2.19, where Q_0 is the H₂ permeability coefficient (mol/m s Pa^{0.5}), E is the H₂ permeation activation energy (J/mol), T is the temperature (K), R is the gas constant (J/mol K), and l is the membrane thickness (m) (She *et al.*, 2014).

$$J = \frac{Q_0 \exp(-E/RT)}{l} \left(\sqrt{P_{H_2, f}} - \sqrt{P_{H_2, p}} \right) \quad (2.19)$$

2.3.4 Graham's Law of Effusion

Graham's law of effusion was formulated by physical chemist Thomas Graham. Graham found experimentally that the rate of effusion of a gas is inversely proportional to the square root of the mass of its particles. This formula can be written as in Equation 2.20.

$$\frac{Rate_1}{Rate_2} = \sqrt{\frac{M_2}{M_1}} \quad (2.20)$$

where:

$Rate_1$ is the rate of effusion of the first gas

$Rate_2$ is the rate of effusion for the second gas

M_1 is the molar mass of gas 1

M_2 is the molar mass of gas 2

Graham's law states that the rate of effusion or of diffusion of a gas is inversely proportional to the square root of its molecular weight. Thus, if the molecular weight of one gas is four times that of another, it would diffuse through a porous plug or escape through a small pinhole in a vessel at half the rate of the other.

Graham's law is most accurate for molecular effusion which involves the movement of one gas at a time through a hole. It is only approximate for diffusion of one gas in another or in air, as these processes involve the movement of more than one gas.

Graham's Law can also be used to find the approximate molecular weight of a gas if one gas is a known species, and if there is a specific ratio between the rates of two gases. The equation can be solved for the unknown molecular weight as shown in Equation 2.21 (Petrucci *et al.*, 2002).

$$M_2 = \frac{M_1 (Rate_1)^2}{(Rate_2)^2} \quad (2.21)$$

2.4 Transport of Hydrogen Through Steel

Hydrogen transport through steel depends on many factors: a reaction occurring on the steel surface, a reaction occurring in the steel, the isotope of the

diffusing substance, structure of steel, and surface of steel. Furthermore, hydrogen permeability, diffusivity, and solubility are the three important hydrogen transport coefficients which involve an understanding of the transport of hydrogen also.

2.4.1 Mechanism of Hydrogen Transport Through Steel

Hydrogen permeation in metals and alloys is a complicated phenomenon including several successive stages: adsorption of hydrogen molecule upon the surface, dissociation into hydrogen atoms, dissolution of adsorbed hydrogen atoms, diffusion through the metal of adsorbed hydrogen atoms, recombination into hydrogen molecule, and desorption. It is a general opinion that the surface processes play an important role in the gas permeation through metals and alloys since it is considered that they are much faster than the diffusion itself (Addach *et al.*, 2005).

In addition to its diffusion through the bulk metal, the permeation of hydrogen through steels involves its entrance at one surface and its exit at another surface of the specimen. There are seven postulated steps that take place before the hydrogen is detected on the output side of the specimen. The permeation of hydrogen through a metallic membrane essentially involves the consecutive steps as shown in Figure 2.7.

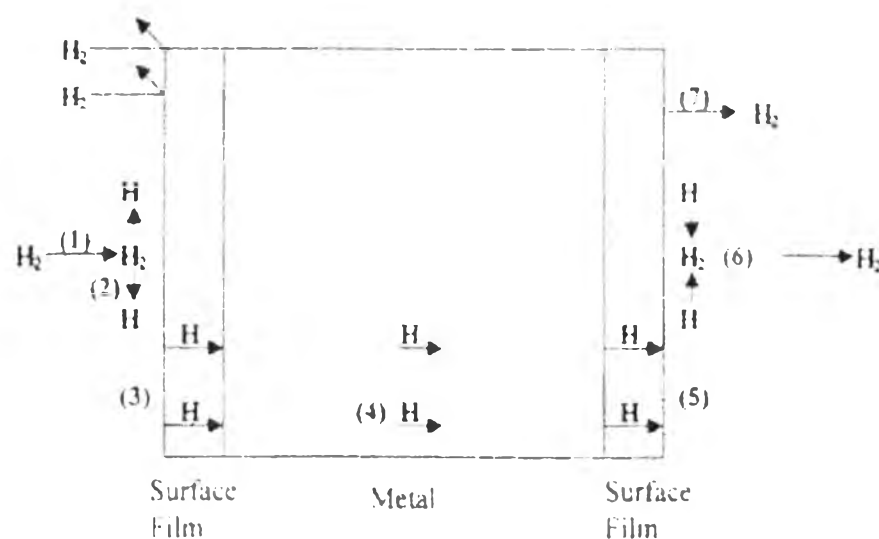


Figure 2.7 Seven steps of hydrogen permeation (Stone, 1981).

This model indicates that there are seven steps in the permeation of hydrogen through a metallic membrane with the presence of surface films at both sides of surfaces. They are:

1. Adsorption of the hydrogen molecule from the gas phase to the surface (Van der Waals adsorption).
2. Dissociation of the molecule to single atoms or adsorbed atoms on the surface (chemisorption).
3. Permeation of adsorbed atoms from the surface to the bulk of the metal through surface film (dissolution of gas in the metal).
4. Diffusion of atoms through the metal under the concentration gradient established.
5. Permeation of atoms through the film on the output side.
6. Recombination of atoms to form hydrogen molecule on the surface.
7. Desorption of the hydrogen molecule from the surface.

In principle, any one of the above seven steps might be sufficiently slow to become the rate-determining or limiting step. Generally, for thin membranes, the rate of permeation is diffusion-controlled which refers to step 4 as the slowest step. Since the above steps are consecutive, the rates at which all the others proceed will become equal to the diffusion rate when the steady state is reached. If the kinetics of the other processes are inherently more rapid than the diffusion step, equilibrium of the surface concentrations on either side of the membrane will be established with the respective gas pressures (Gorman and Nardella, 1962).

2.4.2 Hydrogen Diffusion in Stainless Steel

Stainless Steel (SS) 316, or 316 SS, is an austenitic steel that is commonly used in components of nuclear fission and fusion reactors. Reports on hydrogen-isotope permeation through 316L SS or 316 SS are found in the literature. However, the deuterium permeation has only been studied by a few authors.

In 2014, Lee *et al.* investigated the deuterium transport and isotope effects in type 316L stainless steel over a wide temperature range of 350-850 °C for nuclear fusion and nuclear hydrogen technology applications. They reported that the

deuterium permeability, diffusivity, and solubility obtained for 316L SS were shown in Equations 2.22-2.24.

$$\phi_{D_2} = 4.56 \times 10^{-7} \exp(-71.2 \times 10^3 / RT) \quad (2.22)$$

$$D_{D_2} = 13.8 \times 10^{-7} \exp(-57.5 \times 10^3 / RT) \quad (2.23)$$

$$S_{D_2} = 0.33 \times \exp(-13.7 \times 10^3 / RT) \quad (2.24)$$

In their study, they also obtained the hydrogen permeability, diffusivity, and solubility of 316L SS as shown in Equations 2.25-2.27.

$$\phi_H = 5.25 \times 10^{-7} \exp(-68.9 \times 10^3 / RT) \quad (2.25)$$

$$D_H = 12.4 \times 10^{-7} \exp(-55.1 \times 10^3 / RT) \quad (2.26)$$

$$S_H = 0.42 \times \exp(-13.8 \times 10^3 / RT) \quad (2.27)$$

where ϕ_{D_2} , ϕ_H ($\text{mol m}^{-1} \text{s}^{-1} \text{Pa}^{-0.5}$) are the deuterium and hydrogen permeability of 316L SS, respectively. D_{D_2} , D_H ($\text{m}^2 \text{s}^{-1}$) are the diffusivities of deuterium and hydrogen, and S_{D_2} , S_H ($\text{mol m}^{-3} \text{Pa}^{-0.5}$) are the corresponding solubilities. R ($\text{J mol}^{-1} \text{K}^{-1}$) is the gas constant of 8.314472, and T (Kelvin) is the absolute temperature (Lee *et al.*, 2014).

In 1988, Grant *et al.* studied the flow of hydrogen through 316 SS and the corresponding surface reactions. They found that the flow of hydrogen is strongly influenced by the surface reactions. Moreover, the permeation and diffusion coefficients were obtained by Equations 2.28 and 2.29, respectively.

$$\phi_H = (8.1 \pm 0.7) \times 10^{-7} \exp(- (8.19 \pm 0.08) \times 10^3 / T) \quad (2.28)$$

$$D_H = (7.3 \pm 0.9) \times 10^{-7} \exp(- (6.30 \pm 0.11) \times 10^3 / T) \quad (2.29)$$

where ϕ_H is the permeation coefficient in [$\text{mol m}^{-1} \text{s}^{-1} \text{Pa}^{-0.5}$], D_H is the diffusion coefficient in [$\text{m}^2 \text{s}^{-1}$], and T is the absolute temperature in [K] (Grant *et al.*, 1988).

The hydrogen permeability of stainless steel is also reported in the work of Gunter *et al* (1987), which indicated that stainless steel has wide range of hydrogen permeability at a temperature as shown in Figure 2.8.

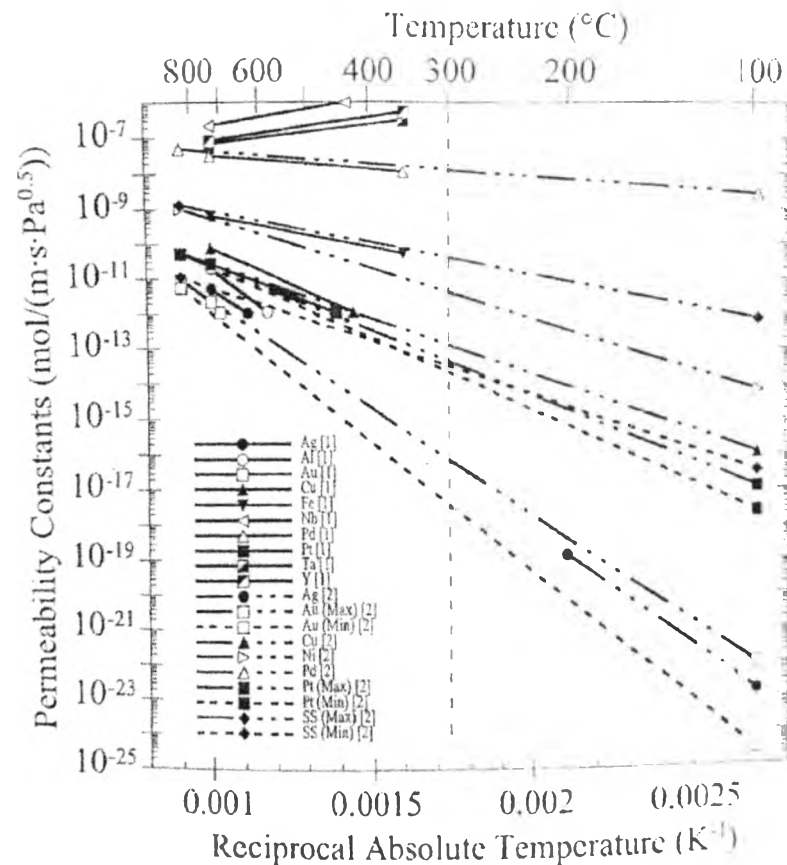


Figure 2.8 Hydrogen permeability constants in various metals as a function of temperature (Gunter *et al.*, 1987).

2.4.3 Hydrogen Diffusion in Carbon Steel

Carbon steel (CS) is a material considered for making a container, like a carbon steel tank. It can be alloyed, singly or in combination, with chromium, nickel, copper, molybdenum, phosphorous, and vanadium in the range of a few percent or less to produce low-alloy steels. There are many types of carbon steel, like CS 1010, CS 1035, and etc., which are different in strength also. However, the most important attribute is much better resistance to atmospheric corrosion than obtained in the low alloys.

In 1979, Gadgeel and Johnson performed hydrogen permeation and diffusion measurement in various types of carbon steel from 500 to 900 K to study the effect of carbon content in the steels. The result shown that different types of

carbon steel have different permeability, diffusivity, and solubility as well as shown in Equations 2.30-2.47.

Carbon steel 1035

$$\phi = 8.076 \times 10^{-6} \exp(-36.160/RT) \quad (2.30)$$

$$D = 1.910 \times 10^{-3} \exp(-11.530/RT) \quad (2.31)$$

$$S = 4.228 \times 10^{-3} P_{H_2}^{1.2} \exp(-24.630/RT) \quad (2.32)$$

Carbon steel 1010

$$\phi = 7.715 \times 10^{-6} \exp(-34.180/RT) \quad (2.33)$$

$$D = 1.700 \times 10^{-3} \exp(-9.480/RT) \quad (2.34)$$

$$S = 4.538 \times 10^{-3} P_{H_2}^{1.2} \exp(-24.700/RT) \quad (2.35)$$

Carbon steel 1020

$$\phi = 8.450 \times 10^{-6} \exp(-35.070/RT) \quad (2.36)$$

$$D = 2.370 \times 10^{-3} \exp(-11.530/RT) \quad (2.37)$$

$$S = 3.565 \times 10^{-3} P_{H_2}^{1.2} \exp(-23.540/RT) \quad (2.38)$$

Carbon steel 1050

$$\phi = 4.700 \times 10^{-6} \exp(-34.130/RT) \quad (2.39)$$

$$D = 2.530 \times 10^{-3} \exp(-13.030/RT) \quad (2.40)$$

$$S = 1.858 \times 10^{-3} P_{H_2}^{1.2} \exp(-21.100/RT) \quad (2.41)$$

Carbon steel 1065

$$\phi = 3.590 \times 10^{-6} \exp(-34.730/RT) \quad (2.42)$$

$$D = 2.440 \times 10^{-3} \exp(-13.190/RT) \quad (2.43)$$

$$S = 1.471 \times 10^{-3} P_{H_2}^{1.2} \exp(-21.540/RT) \quad (2.44)$$

Carbon steel 1095

$$\phi = 2.328 \times 10^{-6} \exp(-33.430/RT) \quad (2.45)$$

$$D = 2.475 \times 10^{-3} \exp(-14.150/RT) \quad (2.46)$$

$$S = 0.941 \times 10^{-3} P_{H_2}^{1.2} \exp(-19.280/RT) \quad (2.47)$$

where ϕ ($\text{cm}^3(\text{NTP})/\text{cm s Pa}^{1.2}$) is the hydrogen permeability, D ($\text{cm}^2 \text{ s}^{-1}$) is the hydrogen diffusivity, and S ($\text{cm}^3 \text{H}_2 \text{ cm}^{-3} \text{metal}$) is the corresponding solubility. R (J

$\text{mol}^{-1} \text{K}^{-1}$) is the gas constant of 8.3144, and T (Kelvin) is the absolute temperature (Gadgeel and Johnson, 1979).

In 1980, Robertson and Thompson studied permeation measurements of hydrogen trapping in 1045 steel. They reported hydrogen permeability in carbon steel 1045 as shown Figure 2.9.

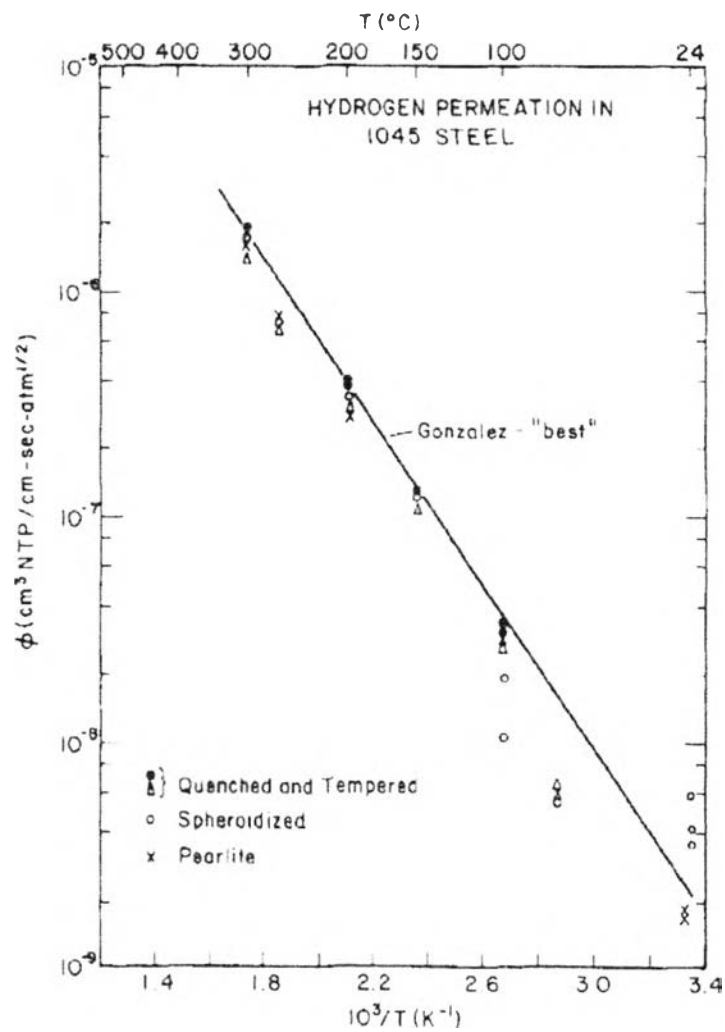


Figure 2.9 Hydrogen permeability in 1045 steel as a function of temperature (Robertson and Thompson, 1980).

In 2014, Kongvarhodom studied the diffusion of hydrogen through carbon steel A106-B pipe at 200 °C, 250 °C, and 300 °C. Carbon steel A106-B is a

representative material for many pipelines and pressure components in the nuclear industry, pulp and paper mills and petroleum refineries. Its chemical composition is shown in Table 2.1.

Table 2.1 Elemental content of carbon steel A106-B (mass fraction in %; balance Fe)

C	Si	Mn	P	S	Cr	Mo
0.20	0.31	0.62	0.02	0.012	0.019	0.004

Moreover, she reported that the hydrogen permeability, and diffusivity obtained for CS A106-B were as in Equations 2.48 and 2.49.

$$\phi = 1.860 \times 10^{-8} \exp(-32.924/RT) \quad (2.48)$$

$$D = 1.273 \times 10^{-7} \exp(-9.373/RT) \quad (2.49)$$

where ϕ ($\text{mol m}^{-1} \text{s}^{-1} \text{Pa}^{-0.5}$) is the hydrogen permeability, D ($\text{m}^2 \text{s}^{-1}$) is the diffusivity of hydrogen, R ($\text{J mol}^{-1} \text{K}^{-1}$) is the gas constant of 8.314472, and T (Kelvin) is the absolute temperature (Kongvarhodom, 2014).

2.5 Hydrogen Effusion Probe (HEP)

The HEP consists of a silver cup, connected via silver and stainless steel tubing to a valve, pressure transducer, vacuum pump, and includes a data acquaintance system. In order to avoid the loss of hydrogen from the device, high purity silver is used due to the low permeation rate of hydrogen through this metal at high temperatures (Steward, 1983). When the cup is sealed to the vessel wall a vacuum tight seal is achieved. The pump is used to create a vacuum within the cup and tubing. The valve, when closed, maintains the vacuum. Hydrogen effusing through the vessel wall is collected within the system, resulting in an increase in absolute pressure. A pressure transducer measures the hydrogen pressure. The system is re-evacuated once a predetermined pressure set-point is reached; 2000 Pa is recommended (McKeen *et al.*, 2007). The data from the pressure transducer is used

to calculate corrosion rate. Multiple thermocouples provide data to allow for temperature compensation of the calculated corrosion rate. A data acquisition and control system is used to control the vacuum pump and valve operation and to record readings from the pressure transducer and thermocouple (McKeen *et al.*, 2010). A schematic of the hydrogen effusion probe components is shown in Figure 2.10.

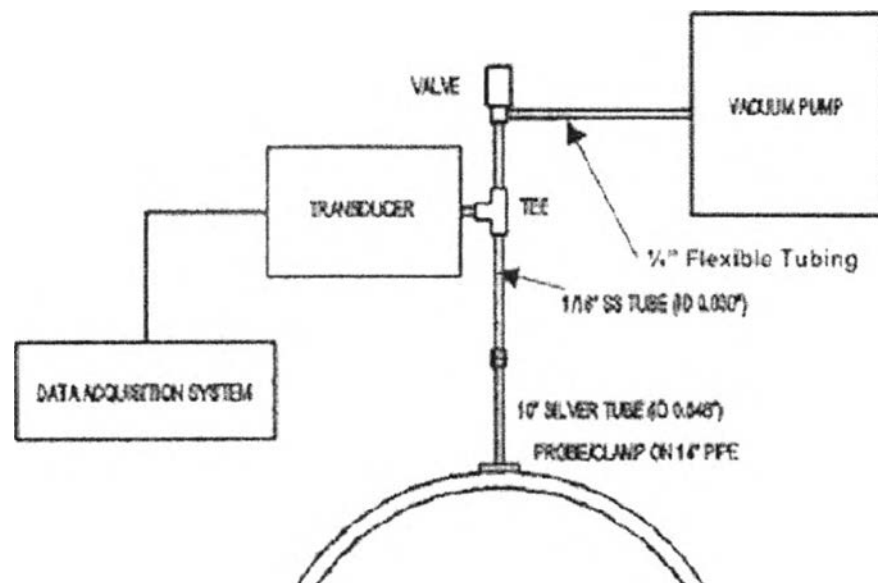


Figure 2.10 Schematic of the hydrogen effusion probe components (McKeen *et al.*, 2007).

2.5.1 Hydrogen Probe Principle

The HEP can measure the pipe thinning rate since the quantity of hydrogen effusing through the carbon steel pipe is proportional to the rate that iron is lost into solution as a consequence of FAC. Once the corrosion process has occurred, one of the products is hydrogen atom. These generated hydrogen atoms diffuse through the carbon steel pipe and are liberated at the exterior surface. They then recombine to hydrogen gas which is collected in the sealed chamber outside of the pipe wall, which causes the increase in pressure. The pressure transducer measures the hydrogen pressure rise which can be used to calculate the wall thinning rate.

The feeder thinning occurs because iron atoms (Fe^{2+}) produced by corrosion of steel dissolve into the coolant as a consequence of FAC. It is assumed that all of the hydrogen liberated in the corrosion reaction diffuses through the pipe wall and one mole of hydrogen gas is produced from one mole of iron losses. The reaction is shown in Equations 2.50 and 2.51.



The rate of corrosion is related to hydrogen evolution and can be determined from the accumulation of hydrogen gas within the chamber according to the Equation 2.52.

$$C_r = \frac{a_c \frac{\partial n_d}{\partial t_d} M_{Fe}}{A_i \rho_{Fe}} \quad (2.52)$$

where:

C_r is the corrosion rate (cm/yr)

a_c is the conversion of days to year (365 days/yr)

$\frac{\partial n_d}{\partial t_d}$ is the daily accumulation of hydrogen gas (mol/day)

M_{Fe} is the molar mass of iron (55.85 g/mol)

A_i is the internal area of pipe (cm^2)

ρ_{Fe} is the density of iron (7.87 g/cm³).

Since hydrogen behaves as an ideal gas at low pressures and moderate temperatures, the number of moles of hydrogen accumulated per day can be related to the change in pressure by the Ideal Gas Law which is shown in Equation 2.53.

$$\frac{\partial n_d}{\partial t_d} = \frac{\partial P_{H_2}}{\partial t_d} \frac{V}{RT_{avg}} \quad (2.53)$$

where:

$\frac{\partial P_{H_2}}{\partial t_d}$ is the rate of pressure increase (Pa/day)

V is the total volume of the HEP (m^3) which depends on the assembly of the HEP

R is the gas constant ($8.314 \text{ m}^3 \cdot \text{Pa} / \text{mol} \cdot \text{K}$)

T_{eff} is the effective temperature in the system (K)

Since various parts of the HEP system are exposed to different temperatures the effective temperature is the sum of the individual temperatures multiplied by their respective volume percentage in the HEP system.

The essential feature of the hydrogen effusion probe is that it is a real-time device, which can detect short-term upsets in the process. By getting near real-time data from corrosion monitoring, operators can relate this data to events that caused the corrosion. Hence, they can lower corrosion rates by adjusting or eliminating corrosion-causing events (Homhuandee, 2008).

2.5.2 Assumptions for Thinning Rate Measurement by the HEP

The requirements for an HEP to be used for the quantitative measurement of FAC rates are as follows (McKeen *et al.*, 2007):

1. The stoichiometric factor relating the rate of atomic hydrogen production to the rate of iron atom oxidation is fixed, and is defined by the reaction:



This means that for every mole of iron lost, one mole of H_2 is produced.

2. All the atomic hydrogen produced by the corrosion process is absorbed locally by the carbon steel experiencing corrosion.

3. All the absorbed hydrogen generated by corrosion diffuses through the wall of the carbon steel pipe, recombines to molecular hydrogen at the external interface, and passes into the gas phase in contact with the external surface.

4. Molecular hydrogen, once formed within the collection volume does not diffuse back through the pipe wall.

5. Any hydrogen dissolved in the electrolyte coolant does not contribute to the hydrogen flux through the wall of the pipe. All of the hydrogen that effuses through the steel comes from the corrosion reaction.

6. A very low concentration of oxidizing species is present in the coolant.

7. Atomic hydrogen does not accumulate at the grain boundaries or at defects.

8. The area over which the collected hydrogen is generated is assumed to be thinning at a uniform rate.

9. The molar mass and density of the carbon steel are assumed to be equal to those of pure iron.